Tracer study of mixing and transport in the upper Hudson River with multiple dams.

*Theodore Caplow[1], Peter Schlosser[2], and David T. Ho[3]

[1]Ph. D. Student, Dept. of Earth & Environmental Engineering, Columbia University, 918 Mudd Building, New York, NY 10027. *Corresponding author. Email tc144@columbia.edu Tel: (212) 854-7065 Fax: (212) 854-7081

[2]Professor, Dept. of Earth & Environmental Engineering, and Professor, Dept. of Earth & Environmental Sciences, Columbia University, New York, NY 10027. Email peters@ldeo.columbia.edu Tel: (212) 854-7065 Fax: (212) 854-7081

[3]Lecturer, Dept. of Earth & Environmental Sciences, and Research Scientist, Lamont-Doherty Earth Observatory, Columbia University, Palisades, New York, NY 10964. Email david@ldeo.columbia.edu Tel: (845) 365-8706 Fax: (845) 365-8155

Abstract

In October 2001, ca. 0.2 mol of SF_6 was injected into the upper Hudson River, a modified natural channel with multiple dams, at Ft. Edward, NY. The tracer was monitored for 7 days as it moved ca. 50 km downriver. The longitudinal evolution of the tracer distribution was used to estimate 1-D advection (9.0 ± 0.2 km d^{-1}) and dispersion (17.3 ± 4.0 m^2 s^{-1}) along the river axis. Comparison of these results to tracer studies on channels without dams suggests that dams reduce longitudinal dispersion below the value expected in a natural channel with the same discharge. SF_6 loss through air-water gas exchange along the river and at two dams (10.7 m combined height) was estimated by observing decay in peak concentration. Losses at dams (approximately 50% per dam) were dominant. The estimated gas exchange at dams was compared to a simple model adapted from those available in the literature. Small amounts of tracer were trapped in a canal segment (ca. 5 km long) that parallels the river, where advection and dispersion were sharply reduced.

Introduction

The evolution of a soluble contaminant or nutrient introduced into a river can be divided into three successive stages, corresponding to periods of vertical, transverse, and longitudinal mixing, respectively (Fischer et al. 1979). The third stage, sometimes referred to as the far-field, begins many river widths downstream of the solute's source, when vertical and transverse mixing are essentially complete. The focus of this contribution is the behavior of solutes in the far-field, a subject of primary concern for estimation of time-of-travel and/or dilution capacity at the watershed or catchment scale (typically tens or hundreds of km).

Predicting the far-field behavior of contaminants in a river requires flow models, and these models, whether analytical or numerical, must be calibrated to accurate observations of stream transport processes. As they affect solutes in the far-field, these processes can be divided into advection (bulk downstream motion), longitudinal dispersion (mixing), and gas exchange (losses or gains of solutes across the air-water interface). Here we describe the measurement of advection, longitudinal dispersion, and gas exchange in a river by means of a deliberately released tracer, sulfur hexafluoride (SF_6).

The experiment covered a 65 km reach of the upper, non-tidal Hudson River between Fort Edward, NY and Troy, NY, and was conducted between October 17 and 23, 2001. This reach has been heavily altered from its natural state by addition of a dredged channel, dams, locks, and canals. A number of industrial facilities and power plants are located along this part of the Hudson, and a public water supply intake is located near the bottom of the study area (at Waterford, NY), underscoring the need for an accurate transport model in the event of a chronic

or sudden release of a toxic contaminant. The experiment described here was the first application of SF_6 tracer to the study area, and among the first large-scale applications of SF_6 to a dammed channel. The goal was to provide basic empirical data on transport in the study area while verifying the SF_6 tracer methodology for applications to other, similar riverine environments.

Previous tracer work in rivers has been performed with fluorescent dyes such as Rhodamine (e.g. Wright and Collings 1964; Lowham and Wilson, Jr. 1971; Atkinson and Davis 2000), although there is a growing body of literature for the application of SF_6 to river studies (e.g. Clark et al. 1994; Clark et al. 1996; Hibbs et al. 1998; Chapra and Wilcock 2000; Ho et al. 2002). SF_6 has several properties that make it preferable to fluorescent dyes for studies of advection and mixing in rivers on large space and time scales. It is non-toxic, inert, inexpensive, and detectable over a large concentration range (the technique used here is sensitive over a concentration range of at least four orders of magnitude from about 10 fmol L^{-1} to about 100 pmol L^{-1}). SF_6 is conservative in the environment and is only lost from the river through gas exchange with the atmosphere.

Study Conditions

The Hudson River flows southward over 500 km from its source in the Adirondack Mountains to New York Harbor, draining an area of 35,000 km^2 (Limburg et al. 1986). The river is navigable downstream of Fort Edward, NY at kilometer point (kmp) 313, measured axially upstream from the southern tip of Manhattan. Below the Federal Dam at Troy (kmp 248), the river is tidal, with bi-directional flow. Above the Federal Dam, the river changes character (Figure 1), becoming a narrower, shallower stream altered from its natural course by the construction of the Champlain Canal system. There are six locks between kmp 248 and kmp 313, for a total change in elevation

of 31 m (Erie 2002). Each lock is 13 m wide and 91 m long and is accompanied by a dam and spillway. Many of the locks are placed at the southern end of man-made canals dug parallel to, but separate from, the natural river. There are four canals in the study area, all located upstream of a lock. These canals, which are approximately 30 m wide, are found above lock #6 (~5 km), lock #5 (~1.5 km), and lock #4 (~0.9 km), and below lock #1 (~0.7 km). The controlling depth for the canals, locks, and navigable river is 3.7 m (12 feet).

The 25-year mean flow of the Hudson River is 147 $m^3 s^{-1}$ at Ft. Edward and 385 $m^3 s^{-1}$ at Troy (USGS 2002; EPA 2000). Major tributaries within this reach include the Batten Kill (kmp 293, average flow 17 $m^3 s^{-1}$), the Hoosic River (kmp 270, average flow 38 $m^3 s^{-1}$), and the Mohawk River (kmp 250, average flow 160 $m^3 s^{-1}$). The mean flow at Ft. Edward during October 2001 was 53 $m^3 s^{-1}$. This volume was the lowest recorded in the past 25 years and is equivalent to 36% and 45% of the annual and October means, respectively. This anomaly is expected to have had a significant effect on rates of advection, dispersion, and gas exchange.

Bathymetry from EPA (2000) was used to estimate the channel width and mean depth at the injection point, as well as the mean properties for the study reach as a whole. The bathymetry consists of mean depth and mean width for a grid that is one box wide in the transverse direction, with a 2 km longitudinal resolution, except between kmp 304 and kmp 313, where the transverse resolution is 3 boxes and the longitudinal resolution is 1 km. The mean width and depth for the upper Hudson River are 268 m and 3.1 m, respectively.

Field Methods

Measurements of SF_6 conducted before the tracer injection indicated a background concentration of less than 10 fmol L^{-1} in the upper Hudson River. On October 17, 2001 at 08:30 EST ("day 0.0"; time is measured in elapsed days since injection), approximately 0.2 moles of SF_6 were bubbled into the river midstream at kmp 311 through a porous rubber/polyethylene tubing (7 m long, 0.6 cm ID, 150 μm pore size). The tubing was wrapped around a metal cylinder attached to a weight and its depth was controlled at approximately 3 m. Flow was maintained for one minute. Shortly thereafter, survey of the SF_6 patch began, using a boat-mounted, fully automated, high-resolution sampling and measurement system (Ho et al. 2002). Water from the river was pumped continuously through a counter-flow membrane contactor, where gases were extracted and analyzed for SF_6 by electron-capture gas chromatography. This equipment takes a concentration measurement every two minutes. Boat speed during surveys ranged from 3 to 8 knots (5 to 15 km h^{-1}), resulting in a spatial data resolution of 0.2 to 0.5 km along the axis of the river.

The survey was conducted for seven consecutive days, between 8 am and 6 pm. The SF_6 patch was surveyed either as the boat traversed the patch in a longitudinal direction upriver or downriver, or from fixed positions as the tracer-tagged water flowed past. In addition to the main patch, a slug of SF_6 trapped in a 5 km canal above lock #6 (kmp 299) was observed for the duration of the experiment.

Analytical Methods

The far-field study of advection and longitudinal dispersion in rivers is often approached via a one-dimensional (1-D) approximation, in which the width and depth are treated as constants, and lateral and vertical mixing are neglected (Fischer et al. 1979; Rutherford 1994). This approximation is justified if the timescale is sufficiently large such that horizontal and vertical mixing are essentially complete before measurements of longitudinal dispersion are made. If a tracer injection is used, it is further necessary that the injection be nearly "instantaneous" in comparison with the timescale of observation.

The transverse scale is much larger than the vertical scale in most rivers, including the upper Hudson. A test of transverse mixing time against longitudinal measurement interval, if successful, suffices to justify the 1-D approximation in non-saline rivers (where vertical water column stratification is assumed to be transient and/or weak). Rutherford (1994) performs this test by assuming a constant dispersion coefficient and estimating transverse mixing time T_t:

$$T_t = \alpha \frac{B^2}{K_y} \tag{1}$$

where B is the mean width of the river (225 m at the injection site), K_y is the transverse dispersion coefficient, and α is a coefficient defining the well mixed state. According to Fischer et al. (1979), if α is set to 0.075 then the tracer concentration will be within 10% of its mean anywhere on the cross-section after an elapsed time of T_t (since injection). The analytical prediction of K_y remains unsatisfactory to many investigators (e.g. Heard et al. 2001; Boxall and Guymer 2003) but $K_y = 0.6\ H\ u^*$ is an expression commonly used for slightly meandering channels (Fischer et al. 1979), where H is mean channel depth (2.6 m at the injection site) and u^*

is the shear velocity. The analytical determination of u^*/u is beyond the scope of this discussion, but for the present purpose a value of 0.10 is appropriate (Fischer et al. 1979; also supported by empirical data in Deng et al. 2001). Using u = 0.1 m s^{-1} (9 km d^{-1}, derived from this study), T_t was found to be 65 h. The first survey of SF_6 concentration used in the calculation of longitudinal dispersion took place 54 h after injection, but the flow passed over two dams during this period, accelerating mixing and lending a high degree of confidence to the assertion that transverse mixing was essentially complete by the time of the first survey.

All measurements used for the calculation of advection, longitudinal dispersion, and gas exchange were made in reaches of the river that were free from sudden changes in width, depth, or cross-sectional area. The ratio of the injection time (1 min) to the time required to complete the shortest profile used in data analysis (1 h) justifies the representation of the injection as "instantaneous" with regard to large-scale transport at this timescale. These facts, together with the mixing argument presented above, enable derivation of meaningful results from the treatment of the injected SF_6 by the idealized 1-D advection-dispersion equation (Taylor 1954; Levenspiel & Smith 1957; Fischer et al. 1979; Rutherford 1994):

$$\frac{\partial c}{\partial t} + u\frac{\partial c}{\partial x} = K_x\frac{\partial^2 c}{dx^2} - \lambda c \qquad (2)$$

where u is the mean advection, K_x is the longitudinal dispersion coefficient, and λ is the first order loss term due to air-water gas exchange. Solving Equation (2) yields:

$$c(x,t) = \frac{\nu M}{A\sqrt{4\pi K_x t}}\exp\left[-\frac{(x-ut)^2}{4K_x t} - \lambda t\right] \qquad (3)$$

where v is the specific volume of the gas tracer, M is the mass of trace gas injected and A is the mean cross-sectional area of the river (all three of these values are constant for the purposes of this analysis). One method for determining K_x from experimental data is via the "change of moment" (Fischer et al. 1979; Rutherford 1994):

$$K_x = \frac{1}{2}\left(\frac{d\sigma^2}{dt}\right) = \frac{1}{2}\left(\frac{\sigma_2{}^2 - \sigma_1{}^2}{t_2 - t_1}\right) \quad (4)$$

where $\sigma_1{}^2$ and $\sigma_2{}^2$ are the variances (second moments) of the tracer distributions at times t_1 and t_2 respectively. Equation (4) is applied between SF_6 surveys, taken on different days, to calculate a single mean value of K_x for the temporal and spatial extent of the study.

The value of σ^2 for the SF_6 patch from a single survey was estimated by fitting Gaussian curves (minimizing chi square) to two longitudinal profiles of the patch, taken very close together in time but in opposite directions, and averaging σ^2 from both curve fits. Bi-directional profiles were used to reduce uncertainty and to remove any possible bias from lag or memory effects in the sampling equipment. The maximum discrepancy between observed values for σ^2 within a single pair of bi-directional profiles was 10%. Four profiles suitable to the fitting of Gaussian curves were collected (a bi-directional pair on both day 3 and day 4). In addition, three pairs of bi-directional profiles were collected in the canal above lock #6 (on days 2, 3, and 4) and analyzed for dispersion by the same method. This approach corresponds to the simplest analytical model, which is symmetrical and constant (i.e. Fickian) dispersion. More complex models are also in use, in particular the "dead zone model", attributed to Hays (1966), which accounts for an asymmetrical tracer patch (with longer upstream tail) by proposing that portions of the river, or its bed, retard pockets of tracer while the rest is advected downstream. The SF_6

profiles from the present study display a slight asymmetry, but the upstream tails were truncated by dams, as it was not possible to survey continuously past these structures.

Equation (4) requires a set of observations of σ^2, each of which is assumed to be synoptic. The data were normalized to a synoptic form by shifting each data point a small distance, determined by the mean advection (u) and the elapsed time between data collection at that point and the time when the peak SF_6 concentration was observed. The maximum shift was < 0.1 σ, where σ^2 was the variance of the profile. Dispersion during the profile itself was neglected.

Loss of SF_6 via gas exchange at the air-water interface was investigated by examining the decline, between successive observations, of the peak SF_6 concentration in the tracer patch. (This approach was chosen because the collection of complete SF_6 inventories, from which losses could be directly calculated, was only possible on one occasion due to interference from locks and dams.) Fischer et al. (1979) observed that in a 1-D system with symmetrical Fickian dispersion and no losses the evolution of the peak concentration (c_p) is proportional to the inverse of the square root of the elapsed time since injection: $c_p \propto t^{-0.5}$. This conclusion is evident from a consideration of Equation (3) at the peak ($x = ut$) with no losses ($\lambda = 0$). If such a tracer peak is measured at two times t_1 and t_2 then it follows directly that:

$$\frac{c_{p2}}{c_{p1}} = \left(\frac{t_1}{t_2}\right)^{0.5} \tag{5}$$

where c_{p1} and c_{p2} are the peak tracer concentrations at times t_1 and t_2, respectively. For the purpose of evaluating net tracer loss from peak concentration data it is useful to introduce f_{12}, the fraction of tracer which is removed from the water between times t_1 and t_2:

$$f_{12} = 1 - \frac{c_{p2}}{c_{p1}} \left(\frac{t_2}{t_1} \right)^{0.5} \quad (6)$$

Equation (6) does not depend upon the actual form or temporal distribution of the losses, provided that the tracer profiles at both t_1 and t_2 are well represented by the Gaussian curves described by Equation (3), and that Equation (5) is valid. Jobson (1997) performed regression analysis on a heterogeneous data set of 422 cross-sections from 60 rivers in the United States and found that $c_p \propto t^{-0.89}$, whereas various other investigators have found values for the exponent ranging from −0.7 to −1.0. This increase in longitudinal dispersion above the intensity suggested by the Fickian model is usually ascribed to additional modes of mixing (e.g. dead zones). The simpler relationship $c_p \propto t^{-0.5}$ was adopted here for two reasons. First, this relationship maintains consistency with the Fickian model used for the dispersion calculations, which appears the most generic model for observing first-order transport effects under these conditions. Second, this relationship matches the observed decay of the SF_6 peak in an inter-dam reach of the study area about 35 km downstream of the injection point (see Results), indicating that the impact of patch asymmetry was minor for the experiment described. Considering the potential for gas exchange losses over this reach, it appears the appropriate exponent relating c_p and t may have been even higher than −0.5, a result at odds with the aforementioned regressions from the literature.

Equation (6) was applied to data from three surveys where c_p was well defined (one each on days 2, 3, and 5) to evaluate the effect of dams upon SF_6 losses to the atmosphere. A large increase in gas exchange is expected at dams, due to the extreme turbulence, bubble invasion, and vertical mixing that occur downstream (e.g. Cirpka et al. 1993; Asher et al. 1996). The reach between the

survey locations for days 2 and 3 is regular in form and unobstructed. Two dams (4.8 m and 5.9 m; Erie 2002) are located between the survey locations for days 3 and 5.

A minor correction was made to f_{12} to account for dilution from tributaries (20% over this reach; EPA 2000). This dilution was assumed to cause a linear reduction in c_p as a function of distance downstream from the injection point.

Results

SF_6 was measured in the river until day 6, at which time the signal of the main patch had decreased to nearly undetectable levels. The downstream motion and longitudinal spreading of the SF_6 peak is well represented in the data, despite irregularities in the river (locks and dams). Results from a longitudinal profile taken on day 3 (Figure 2) clearly indicate small slugs of tracer trapped in canals at locks #5 and #6, as well as the main tracer patch further downstream. The SF_6 mass inventory in the main channel on day 3 was estimated as 1.5 ± 0.15 mmol, approximately 1% of the estimated amount injected. Based on prior experience (Ho et al. 2002) and the relatively shallow depth of the river, it is expected that the majority of the SF_6 injected (more than 90%) escaped from the water as bubbles during the injection process. Additional reduction in the SF_6 inventory is attributed to air-water gas exchange, including losses at dams.

Advection

Observations of the peak concentrations within the tracer patch enabled estimates of the mean advection rate (Figure 3). Mean advection over a 42 km reach (kmp 306 to kmp 264) was 9.0 ± 0.2 km d^{-1} (0.104 ± 0.002 m s^{-1}), corresponding to a transit time of seven days from Fort Edward

to Troy (65 km) if the same rate is applied to the remaining 23 km. Multiplying the observed advective rate by the cross-sectional area of the river at the injection point just south of Ft. Edward (585 m^2) yields a flow rate of 61 $m^3\ s^{-1}$. This rate is in reasonable agreement with the rate of 53 $m^3\ s^{-1}$ reported by the USGS at Ft. Edward for the whole of October 2001.

Dispersion

On day 2 (at kmp 289) and day 3 (at kmp 280) it was possible to obtain pairs of bi-directional profiles of the main body of the SF_6 patch suitable for extracting the variance (σ^2) by fitting a Gaussian curve to each profile (Figure 4). The variances for each pair were averaged and the longitudinal dispersion coefficient (K_x) was calculated using Equation (4), resulting in values of $15.7 \pm 2.0\ m^2\ s^{-1}$ for day 2.3 (55 h from injection) and $19.0 \pm 2.4\ m^2\ s^{-1}$ for day 3.2 (77 h from injection). The average K_x was $17.3 \pm 4.0\ m^2\ s^{-1}$ ($1.50 \pm 0.35\ km^2\ d^{-1}$). The data supporting this value were collected along the top 31 km of the study reach. Downstream of kmp 280, no further determinations of σ^2 were possible. In this lower reach (kmp 280 to kmp 248), significant changes in the character of the channel or the volume of the flow are not evident, suggesting that the estimate of K_x obtained from the upper reach should be a reasonably good approximation for this region as well.

Gas Transfer

Results from applying Equation (6) to three successive pairs of peak tracer concentration measurements are shown in Table 1. According to these limited results, the dams are the major cause of SF_6 tracer loss in the study area, and SF_6 losses between dams are a very small term in the overall loss rate. No detectable loss was measured over a 9 km reach (measurements were 23

h apart) between kmp 289 and kmp 280 that contained no dams, but a 72% loss was recorded over a 14 km reach (measurements were 39 h apart) between kmp 280 and kmp 266 that contained two dams.

SF_6 trapped in the canal above lock #6

The mean cross sectional area of the canal above lock #6 was estimated (field observations) to be 90 ± 25 m^2. The total SF_6 inventory in this canal was calculated from a profile taken on day 3 (3.1 days after injection) as 72 ± 13 μmol (using a cross-sectional area of 90 m^2). This inventory is approximately 5% of the inventory measured in the main channel on day 3. Tracer mass in the canal was also calculated from profiles on days 2 and 4 (Figure 5), but the data do not show a significant trend that would enable an estimate of gas transfer rate. Gaussian curves were fitted to each profile (Figure 5). Advection was determined from the peaks of the curve fits to be 0.7 ± 0.06 km d^{-1}. Longitudinal dispersion (K_x) in the canal was estimated as 1.2 ± 0.3 m^2 s^{-1} (0.11 ± 0.025 km^2 d^{-1}) by a least square fit of σ^2 versus time, corresponding to the relationship predicted by Equation (4).

Discussion

The advection rate along the measured reach was constant within measurement errors (Figure 3). Intuitively, this result seems surprising in view of the irregularities along this reach. To examine the uniformity of flow per unit area, cross-sectional area and average contributions from tributaries were obtained from EPA (2000) and plotted versus river kilometer (Figure 6). The plot illustrates that as tributaries and run-off enter the main stem of the river, the cross-sectional area increases to accommodate the additional flow, producing a near-constant mean velocity.

Deng et al. (2001) compile a set of 73 empirical data points containing longitudinal dispersion coefficient, width, depth, mean velocity, and shear velocity, drawn from studies of 29 different rivers in the United States. The data set, derived primarily from dye tracer studies, contains 58 data points from Seo and Cheong (1998) and 15 data points from Rutherford (1994). These measurements were made on reaches without dams. As no similar data set exists for rivers with dams, the Deng et al. (2001) data is used here as a means for comparing the upper Hudson River to channels without dams.

The median and mean K_x for all 73 data points are 40.5 and 132 $m^2 s^{-1}$, respectively. 77% of the K_x measurements were higher than that found for the upper Hudson River. These data were used to construct plots of K_x versus nominal discharge (width × depth × mean velocity), mean velocity, and nominal cross-sectional area (width × depth), respectively (Figure 7). Two upper Hudson River data points were added to the plots: the solid circles represent the results of the October 2001 SF_6 study. The solid triangles ("normal-flow prediction") represent the upper Hudson River after applying a correction for the anomalously low flow conditions prevalent during the experiment. An increase by a factor of 2.4 in the discharge of the upper Hudson River during the study would correspond to 25-year mean conditions. Hibbs et al. (1998), on the basis of earlier work by McQuivey and Keefer (1974), suggest that a linear relationship between K_x and discharge is successful within ± 80% in natural streams if at least one measured value of K_x has already been found. Applying a linear factor of 2.4 to K_x in the upper Hudson River results in an increase from 17 to 42 $m^2 s^{-1}$. It is further assumed, for the purposes of this prediction, that the cross-sectional area would not change significantly with discharge (the dams control cross-

sectional area), but that the mean velocity would increase by an amount proportional to the increase in discharge.

In comparison to the un-dammed channels from the Deng et al. data, K_x in the upper Hudson River (for both the observed and normal-flow cases) falls within or slightly above the range expected from the measured velocity (Figure 7b), but well below the range expected from the discharge (Figure 7a) or nominal cross-sectional area (Figure 7c). It can be generally observed from Figure 7 that K_x is a stronger function of velocity than of cross-sectional area. Taken together, these two points imply that the addition of dams to the upper Hudson River reduced K_x below the values expected from a natural channel of the same discharge. The effect of dams is to increase cross-sectional area and reduce velocity proportionally. The greater dependence of K_x on velocity results in a net reduction of K_x, causing a sharp reduction of K_x below the value expected based on cross-sectional area (Figure 7c). This hypothesis should be verified by further empirical confirmation, e.g. additional tracer studies on dammed channels.

The prediction of K_x from theoretical relationships based upon physical stream parameters was reviewed (e.g. Deng et al. 2001; Deng et al. 2002), as were regressions of peak unit concentration (a measure of longitudinal dispersion normalized by flow rate) against time (Jobson et al. 1997). Although these models offer some promise for un-dammed reaches, none have demonstrated reliable prediction of K_x within a factor of 2 on a river not used for the development of the model. For example, the relationship of Deng et al. (2001) predicts K_x = 69 m^2 s^{-1} for the upper Hudson River under the study conditions (using measured *B, h,* and *u* and

assuming $u^*/u = 0.1$). Despite advances in analytical prediction, tracer studies continue to hold value in the determination of longitudinal dispersion, particularly in dammed channels.

The relatively slow mixing and advection in the canals, together with expected seasonal variance in these properties (as a function of boat traffic and lock cycling rate), is of significance for spill forecasting and modeling. The canals appear to have the capacity to trap small amounts of solutes from the main channel for long periods of time (days to weeks). It follows that contaminants introduced directly into the canals would persist for a much longer time, and at higher concentrations, than they would if spilled in the main channel. Five days into the experiment, parcels of water containing significant amounts of SF_6 were still working their way through the canal above lock #6 (only several km south of the injection point). At this time the main patch had passed 30 km downriver and peak concentrations there were an order of magnitude smaller than in the lock #6 canal.

Predicted Gas Transfer at Dams

Erie (2002) tabulated the change in river elevation at each lock on the upper Hudson; these drops are good estimates for the heights of the dams. Based upon a review of the literature, a rough model was developed (Appendix I) to calculate the loss of SF_6 over the dams of the upper Hudson River as a function of dam height, h, and specific flow, q (flow per unit of dam width). The net flow rate at these dams was calculated as 76 m^3 s^{-1} by adding 24% tributary dilution (EPA 2000) to the flow determined at the injection site from the measured advection. Three values for q were examined, corresponding to 50%, 100%, and 200% of the net flow rate divided by an approximate mean dam width of 200 m (observed from satellite photos). Predicted values for f_{12} from the model (75% – 86%) are compared to the measured (72%) cumulative losses over

the two dams spanned by the tracer patch peak measurements on days 3 and 5 (Table 2). The model developed here is a rough approximation which appears to capture the major effects. A dedicated experiment would be necessary to understand all of the factors affecting gas exchange over dams of this type.

Acknowledgements

We thank Nicholas Santella and Fred Stuart for assistance in the field. Special thanks to John Lipscomb, boat captain for Riverkeeper, whose expert handling of his vessel ensured a smooth and successful field project. The authors are grateful for the valuable comments of three anonymous reviewers. Funding was provided by a generous grant from the Dibner Fund and by the Lamont Investment Fund. LDEO contribution ####.

Appendix I. Model for SF_6 loss over dams on the Upper Hudson River

Both Gulliver et al. (1998) and Cirpka et al. (1993) present predictive relationships found in the literature for gas transfer efficiency as a function of physical parameters of flow over hydraulic structures (dams, weirs, spillways, cascades and gates). It is standard in these relationships to employ the dependent variables E and r:

$$E = 1 - \frac{1}{r}$$
$$r = \frac{C_u - C_e}{C_d - C_e} \tag{A1}$$

where E is the gas transfer efficiency (achieved gas transfer divided by total potential gas transfer), r is termed the excess ratio (or deficit ratio, depending upon the gas), C_e is the equilibrium gas concentration, and C_u and C_d are the gas concentrations upstream and downstream of the structure, respectively.

According to Cirpka et al. (1993) and Gulliver et al. (1998), gas transfer at hydraulic structures of moderate size (1 to 10 m high) is dominated by diffusion across the surface of air bubbles that are entrained as the falling water enters the catch basin below the dam. The formation and division of bubbles greatly magnifies the available surface area for gas transfer, while the physical turbulence in the zone where these bubbles rise to the surface accelerates dispersion away from the bubble-water interface. This process can be parameterized in a number of ways. Gulliver et al. (1998) investigated 12 formulations and settled on the following classical relationship, originally formulated by Avery and Novack (1978), as the best predictor for oxygen invasion at weirs:

$$E_{O_2,weir} = 1 - \frac{1}{1 + 2.4 \times 10^{-5} Fr^{1.78} Re^{0.53}}$$

$$Fr = \left(\frac{8gh^3}{q^2} \right)^{1/4} \quad Re = \frac{q}{\nu} \tag{A2}$$

where $E_{O_2,weir}$ is the gas transfer efficiency for oxygen, *Fr* and *Re* are the Froude and Reynolds numbers of the jet, respectively, *g* is the gravitational constant, *h* is the drop over the weir, *q* is the specific flow per horizontal length of weir ($m^2 s^{-1}$), and ν is the kinematic viscosity of the water (SI units are used for all variables). This relationship was developed for water at 15 ˚C. Over 95% of upper Hudson River water temperature observations from the October 2001 study were within ± 2 ˚C of 15 ˚C.

In order to apply Equation (A2) to SF_6, the difference in molecular properties between O_2 and SF_6 must be considered. Cirpka et al. (1993) show that both O_2 and SF_6 have sufficiently high Henry's Law constants to ensure that gas exchange is limited by the liquid side of the air-water interface, even inside of a rising bubble of entrained air. Their formulation for the excess ratio, *r*, for gases sharing this characteristic takes the form:

$$r = 1 + Y\sqrt{D} \tag{A3}$$

where *Y* is a constant specific to the flow and to the weir, and *D* is the aqueous molecular diffusion coefficient. Designating $R_D = D_{SF_6} / D_{O_2}$ (the ratio of the molecular diffusion coefficients of SF_6 and O_2) and using Equations (A1) and (A3), the SF_6 transfer efficiency can be expressed as a function of E_{O2} and R_D:

$$E_{SF6} = \left(1 + \frac{(E_{O2})^{-1} - 1}{\sqrt{R_D}} \right)^{-1} \tag{A4}$$

In all calculations, R_D is taken as 0.53.

As written, Equation (A2) is intended for oxygen invasion, and therefore Equation (A4) is an estimate for the invasion of SF_6, rather than its evasion (loss). Asher et al. (1996) demonstrate that gas transfer in bubble plumes should not be assumed to be symmetrical with regard to invasion or evasion of a particular gas. Invasive transfer includes a contribution from a certain fraction of bubbles that will collapse completely before surfacing, adding gas to the water in a non-equilibrium process. Evasive transfer lacks this term and therefore will be over-estimated by parameterizations developed from observations of invasion. Asher et al. (1996) point out that this asymmetry will increase with decreasing solubility (because the contribution of a collapsed bubble becomes more significant relevant to the contribution of a surfacing bubble), and also suggest that evasion for highly insoluble gases such as SF_6 will be further reduced (relative to invasion) by depletion of dissolved gas in the immediate vicinity of the rising bubble plume.

Asher et al. (1996) conducted experiments in a seawater tank, revealing that under sufficiently bubbly conditions, transfer efficiency for SF_6 invasion could be up to 50% greater than for SF_6 evasion. However, their results also suggest that the equations derived here from O_2 data can be expected to underestimate SF_6 invasion by roughly the same amount that they overestimate SF_6 evasion; thus the total overestimate of SF_6 loss from a river dam is expected to be substantially less than 50%. The current model is intended to illustrate the effect of various parameters (such as dam height) on gas exchange while providing no more than a crude estimate of the magnitude. Lacking methodical studies of SF_6 loss over dams of the type encountered in the upper Hudson

River, any additional precision would be conjectural at this point. Accordingly, the model neglects asymmetry with regard to direction.

Equation (A2) was originally derived for sharp crested weirs with a separated free jet of water. On the upper Hudson River, the majority of dams were observed to be of the rounded crest type (ogee crest), with an inclined spillway and attached flow. Based on 54 small dams, Butts and Evans (1983) developed a predictive equation for oxygen deficit ratio r that included a shape parameter. As presented in Tang et al. (1995), their equation has the form:

$$r = 1 + b \bullet f(a,h,T) \tag{A5}$$

where a is a factor to account for water quality, h is dam height, T is temperature, and the shape parameter b ranges from 0.6 for a broad-crested dam to 1.05 for a sharp-crested weir. In order to convert transfer efficiencies derived from the sharp-crested weir equation (A2) for use with the broad crested dams of the upper Hudson River, consider two dams of equal height under equal conditions, for which $f(a,h,T)$ is a constant, Z:

$$r = 1 + Zb \tag{A6}$$

Comparing this relationship with the top part of Equation (A1) reveals:

$$E = \left(\frac{1}{Zb} + 1 \right)^{-1} \tag{A7}$$

This equation holds for a dam of either shape. To convert from a sharp weir to a broad crest:

$$\frac{E_{broad}}{E_{weir}} = \left(\frac{1}{Zb_{broad}} + 1 \right) \left(\frac{1}{Zb_{weir}} + 1 \right)^{-1} \tag{A8}$$

which after manipulation yields:

$$E_{broad} = \left[\frac{b_{weir}}{b_{broad}} \left(\frac{1}{E_{weir}} - 1 \right) + 1 \right]^{-1} \tag{A9}$$

Finally, considering that $C_e << C_d < C_u$ for all of the SF_6 concentrations in Table 1 allows Equation (A1) to be restated for SF_6:

$$E_{SF6} = 1 - \frac{C_d}{C_u} = f_{12} \tag{A10}$$

where f_{12} is the loss fraction introduced in the main body of this work. Combining Equations (A10) and (A9) and restating (A4) and (A2) for clarity gives a complete expression for SF_6 extraction efficiency as a function of flow rate q and dam height h:

$$f_{12} = \left[\beta \left(\frac{1}{E_{SF6,weir}} - 1 \right) + 1 \right]^{-1}$$

$$E_{SF6,weir} = \left(1 + \frac{\left(E_{O2,weir}\right)^{-1} - 1}{\sqrt{R_D}} \right)^{-1} \qquad \beta = \frac{b_{weir}}{b_{broad}}$$

$$E_{O2,weir} = 1 - \frac{1}{1 + 2.4 \times 10^{-5} F^{1.78} R^{0.53}} \qquad R_D = \frac{D_{SF6}}{D_{O2}} \tag{A11}$$

$$F = \left(\frac{8gh^3}{q^2} \right)^{1/4} \qquad R = \frac{q}{\nu}$$

where $\beta = 1.75$ and $R_D = 0.53$ as discussed, and values taken for g and ν were 9.81 m s^{-2} and 1.15 x 10^{-6} m^2 s^{-1}, respectively.

It is interesting to note that EPA (2000) make use of Cirpka et al. (1993) as their primary source for modeling volatilization of certain contaminants (PCBs) at these same dams in the upper Hudson River. EPA concluded that PCB losses at each dam were less than 3%, and thus chose to neglect volatilization at dams in their composite PCB model of the upper Hudson River.

Appendix II. References

Asher, W. E., Karle, L. M., Higgins, B. J., Farley, P. J., Monahan, E. C., and Leifer, I. S., (1996). "The influence of bubble plumes on air-seawater gas transfer velocities." *J. Geophy. Res.,* 101(C5), 12027-12041.

Atkinson, T.C. and Davis, P. M., (2000). "Longitudinal dispersion in natural channels: 1. Experimental results from the River Severn, UK." *Hydrol. Earth Syst. Sci.,* 4(3), 345-353.

Boxall, J. B., and Gumer, I. (2003). "Analysis and prediction of transverse mixing coefficients in natural channels." *J. Hydraulic Engrg.* 129(2), 129-139.

Butts, T. A., and Evans, R. L. (1983). "Small stream channel dam aeration characteristics." *J. Environ. Engrg.,* 109(3), 555-573.

Chapra, S. C., and Wilcock, R. J. (2000). "Transient storage and gas transfer in lowland stream." *J. Environ. Engrg.,* 126(8), 708-712.

Cirpka, O., Reichart, P., Wanner, O., Muller, S. R., and Schwarzenback, R. P. (1993). "Gas exchange at river cascades: field experiments and model calculations." *Environ. Sci. Technol.,* 27(10), 2086-2097.

Clark, J. F., Schlosser, P., Stute, M., and Simpson, H. J. (1996). "SF_6-^3He tracer release experiment: a new method of determining longitudinal dispersion coefficients in large rivers." *Environ. Sci. Technol.,* 30(5), 1527-1532.

Clark, J. F.; Wanninkhof, R.; Schlosser, P.; Simpson, H. J. (1994). "Gas exchange rates in the tidal Hudson River using a dual tracer technique." *Tellus*, B46(4), 274-285.

Deng, Z., Singh, V. P., and Bengtsson, L. (2001). "Longitudinal dispersion coefficient in straight rivers." *J. Hydraulic Engrg.,* 127(11), 919-927.

Deng, Z., Bengtsson, L., Singh, V. P., and Adrian, D. D. (2002). "Longitudinal dispersion coefficient in single channel streams." *J. Hydraulic Engrg.,* 128(10), 901-916.

EPA (2000) *Revised Baseline Modeling Report: Hudson River PCBs Reassessment RI/FS* EPA, New York. Available online at http://www.epa.gov/hudson/reports.htm, viewed 02/04/02.

Erie Lock 2 Employees (2002). http://www.yolles.net/canals/pagef.htm, web site viewed 01/20/02.

Fischer, H. B., List, E. J., Imberger, J., Koh, R. C. Y., and Brooks, N. H. (1979). *Mixing in inland and coastal waters*, Academic Press, New York.

Gulliver, J. S., Wilhelms, S. C., and Parkhill, K. L. (1998). "Predictive capabilities in oxygen transfer at hydraulic structures." *J. Hydraulic Engrg.,* 124(7), 664-671.

Hays, J. R. (1996). "Mass transport phenomena in open channel flow." Ph.D. dissertation, Vanderbilt University, Nashville, Tennessee.

Heard, S. B, Gienapp, C. B., Lemire, J. F., Heard, K. S. (2001). "Transverse mixing of transported material in simple and complex stream reaches." *Hydrobiol.* 464, 207-218.

Hibbs, D. E., Perkhill, K. L., and Gulliver, J. S. (1998). "Sulfur hexafluoride gas tracer studies in streams." *J. Environ. Engrg.*, 124(8), 752-760.

Ho, D.T., Schlosser, P. and Caplow, T. (2002). "Determination of longitudinal dispersion coefficient and net advection in the tidal Hudson River with a large-scale, high resolution SF_6 tracer release experiment." *Envir. Sci. Technol.,* 36, 3234-3241.

Hohman, M. S., and Parke, D. B. (1969) in *Hudson River Ecology*, Hudson River Valley Commission of New York, Albany, NY, 60-81.

Jähne, B., Munnich, K. O., Bosinger, R., Dutzi, A., Huber, W., and Libner, P. J. (1987). "On the parameters influencing air-water gas exchange." *J. Geophys. Res.* 92(C2), 1937-1949.

Jobson, H. E. (1997). “Predicting travel time and dispersion in rivers and streams.” *J. Hydraulic Engrg.* 123(11), 971-978.
Kashefipour, S. M. and Falconer, R. A. (2002). “Longitudinal dispersion coefficients in natural channels.” *Water Research,* 36, 1596-1608.
Levenspiel, O. and Smith, W. K. (1957). “Notes on the diffusion-type model for the longitudinal mixing of fluids on flow.” *Chem. Engng. Sci.,* 6, 227-233.
Limburg, K. E., Moran, M. A., and McDowell, W. H. (1986). *The Hudson River Ecosystem*, Springer-Verlag, New York.
Lowham, H. W., and Wilson, Jr., J. F. (1971) "Preliminary results of time-of-travel measurements on Wind/Bighorn River from Boysen Dam to Greybull, Wyoming.", *U. S. Geological Survey Report.*
McQuivey, R. S., and Keefer, T.N. (1974). “Simple method for predicting dispersion in streams.” *J Envir. Engrg. Div.,* ASCE, 100(4), 997-1011.
Rutherford, J. C. (1994) *River mixing*, Wiley, New York.
Seo, I. W., and Cheong, T. S. (1998). “Predicting longitudinal dispersion coefficient in natural streams.” *J. Hydraulic Engrg.,* 124(1), 25-32.
Tang, N. H., Nirmalakhandan, N., and Speece, R. E. (1995). “Weir aeration: models and unit energy consumption.” *J Envir. Engrg.,* 121(2), 196-199.
Taylor, G. I. (1954). “Dispersion of matter in turbulent flow through a pipe.” *Proc. Royal Soc.* Ser. A, 223, 446-468.
USGS (2002) http://water.usgs.gov, web site viewed 02/04/02.
Wright, R. R., and Collings, M. R. (1964). "Application of fluorescent tracing techniques to hydraulic studies." *J. Amer. Water Works Assoc.*, 56, 748-755.

Appendix III. Notation

A = cross-sectional river area;

B = mean river width;

C_d = downstream concentration;

C_e = equilibrium concentration;

C_i = initial concentration;

C_u = upstream concentration;

D = aqueous molecular diffusion coefficient;

E = gas transfer efficiency;

Fr = Froude number;

H = mean river depth;

K_x = longitudinal dispersion coefficient;

K_y = transverse dispersion coefficient;

M = mass of trace gas injected;

Re = Reynolds number;

R_D = ratio of molecular diffusion coefficients;

T = temperature;

T_t = transverse mixing time;

Y, Z = arbitrary constants;

a = water quality factor;

b = dam shape factor;

c = tracer concentration;

c_p = peak tracer concentration;

f_{12} = fraction of tracer lost between observations;

g = gravitational constant;

h = dam height;

q = flow per unit width;

r = excess ratio;

t = time;

t_0 = injection time;

u = mean advective velocity;

u^* = bed shear velocity;

v = specific volume;

x = distance traveled;

α = coefficient defining complete transverse mixing;

β = ratio of dam shape factors;

Δc = air-water concentration difference;

λ = gas exchange loss term;

ν = kinematic viscosity; and

σ^2 = variance (second moment) of a distribution.

Table 1: SF_6 losses with and without dams, calculated from peak concentrations.

Day	*kmp*	σ_{pred}, *km*[a]	*Modeled Peaks, fmol L^{-1}*		*Actual Peak, fmol L^{-1}*	f_{12}	$t_2 - t_1$, *days*	*# of dams* $1 \leftrightarrow 2$
			Dispersion only	*Dispersion & Dilution*				
2.31	288.8	2.63			281			
3.21	279.9	3.10	239	223	222	0.00	0.9	0
4.90	266.1	3.83	193	155	43[b]	0.72	1.7	2

[a]The values given for σ are not the measured values; these are expected values based on the measured mean K_x. This approach is necessary to apply the peak inventory estimate evenly to locations where σ could not be measured directly, as well as those where it could be measured.

[b]The peak was tentatively identified twice more shortly after this time. Both measurements were similar to this one. Following these measurements, the patch crossed another dam and signal levels fell below the detection limit.

Table 2: Net tracer loss over two dams compared with analytical predictions.

kmp	*h, m*	*Predicted f_{12}*			*Cumulative f_{12}*	
		$q=0.19\ m^2s^{-1}$	*$q=0.38\ m^2s^{-1}$*	*$q=0.76\ m^2s^{-1}$*	*Predicted, %*	*Measured, %*
270	4.8	0.59	0.53	0.47	75 - 86	72
267	5.9	0.66	0.60	0.54		

Figure 1. ***Map of the Study Area. Locations of dams are shown as horizontal bars. The inset reveals the canal (5 km long) above lock #6, where a small quantity of tracer was trapped for the duration of the experiment.***

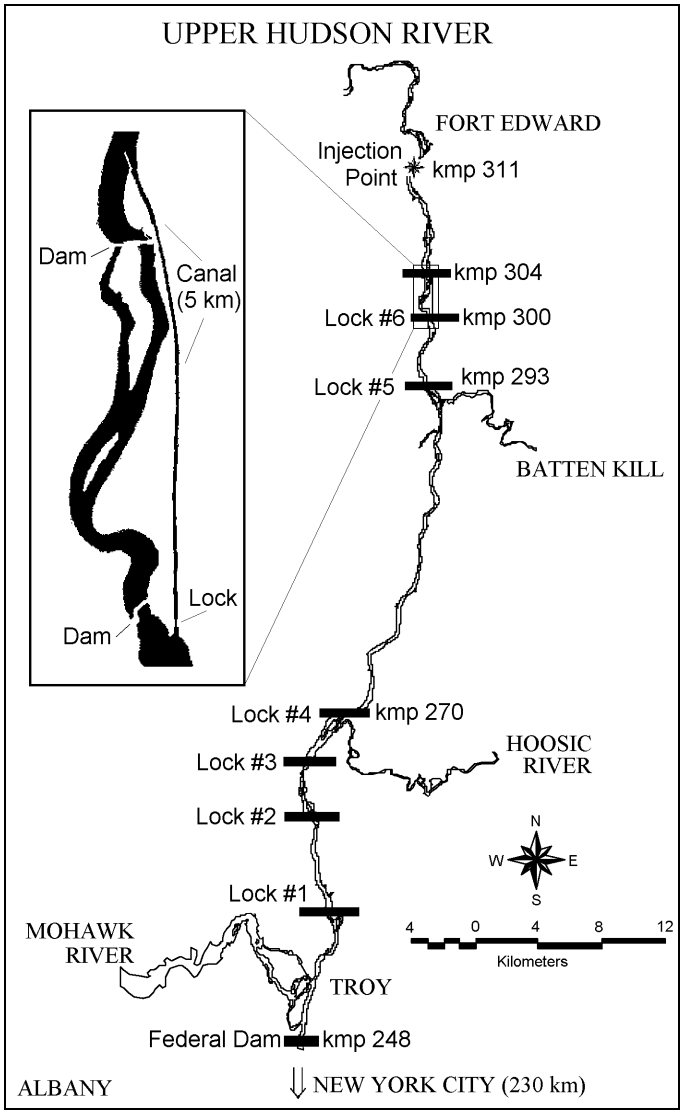

(single column figure)

Figure 2. ***SF_6 tracer concentrations and boat movement for a single, 6-hour profile on day 3. Note that the cross-sectional area of the main channel (leftmost peak) is approximately ten times larger than in the canals (center and rightmost peaks).***

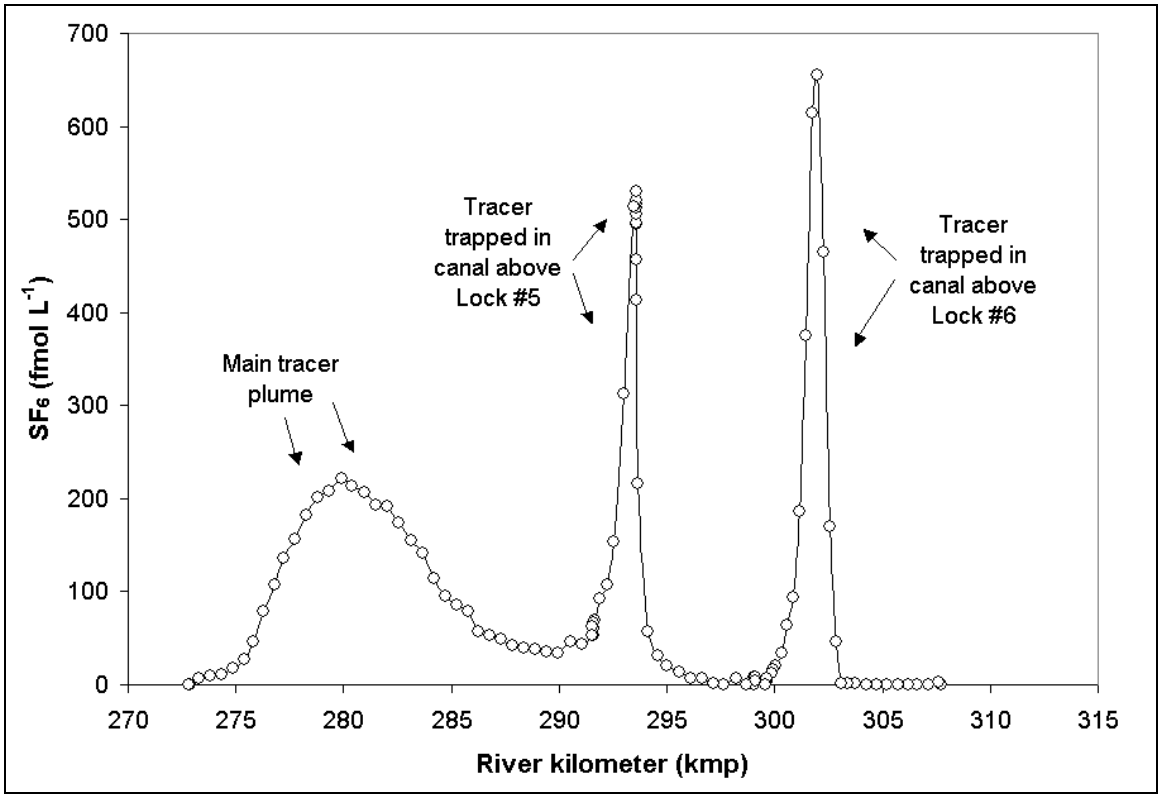

(two column figure)

Figure 3. ***Location of the peak SF_6 concentration vs. time, indicating a nearly constant advective rate of 9 km d^{-1}.***

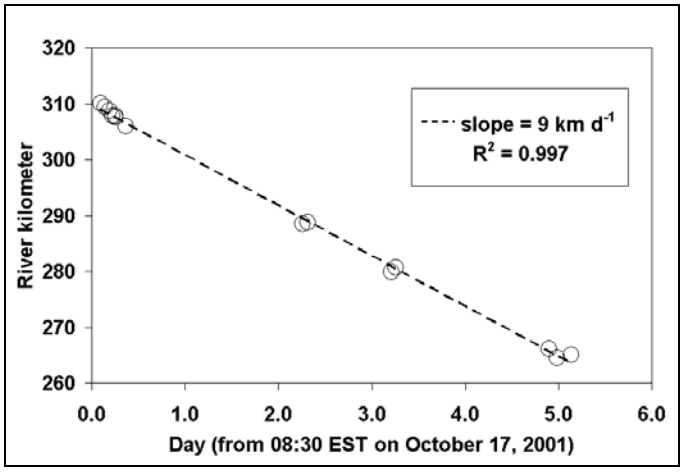

(single column figure)

Figure 4. ***Bi-directional SF_6 patch profiles on days 2 and 3. The longitudinal dispersion coefficient K_x was calculated for each of the surveys from σ^2 according to Equation (4), then averaged.***

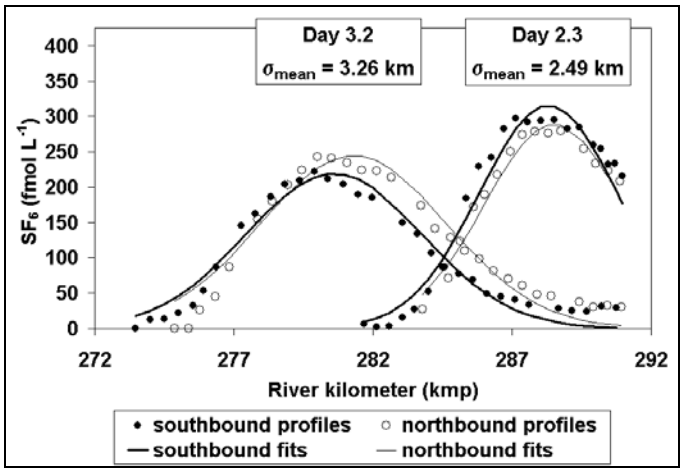

(single column figure)

Figure 5. ***Gaussian curves fit to 3 days of profiles in the canal above lock #6. (For clarity, only northbound profiles are shown). Average inventories from bi-directional profiles are shown above each curve.***

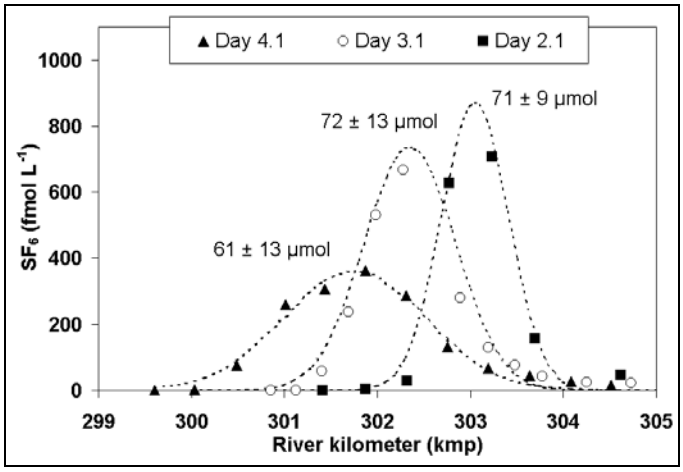

(single column figure)

Figure 6. ***Variation of cross section and flow in the upper Hudson River*** *(bathymetry from EPA 2000).*

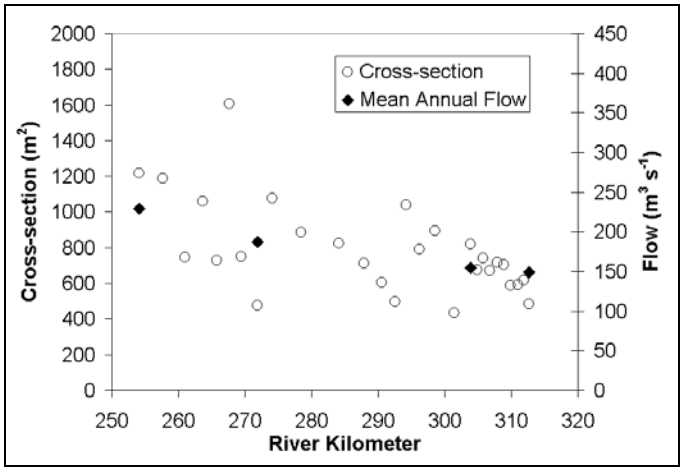

(single column figure)

Figure 7. ***K_x versus (a) nominal discharge, (b) mean velocity, and (c) nominal cross-sectional area for the upper Hudson River, compared with data from Deng et al. (2001). The mean velocity used for the upper Hudson River was 0.10 m s^{-1} (from observed rate of tracer advection). Using this velocity yields a nominal discharge of 86.4 m^3 s^{-1}, somewhat higher than the monthly mean USGS observation at Ft. Edward. Filled circles represent observed values; filled triangles represent values corrected to long-term mean discharge (see text).***

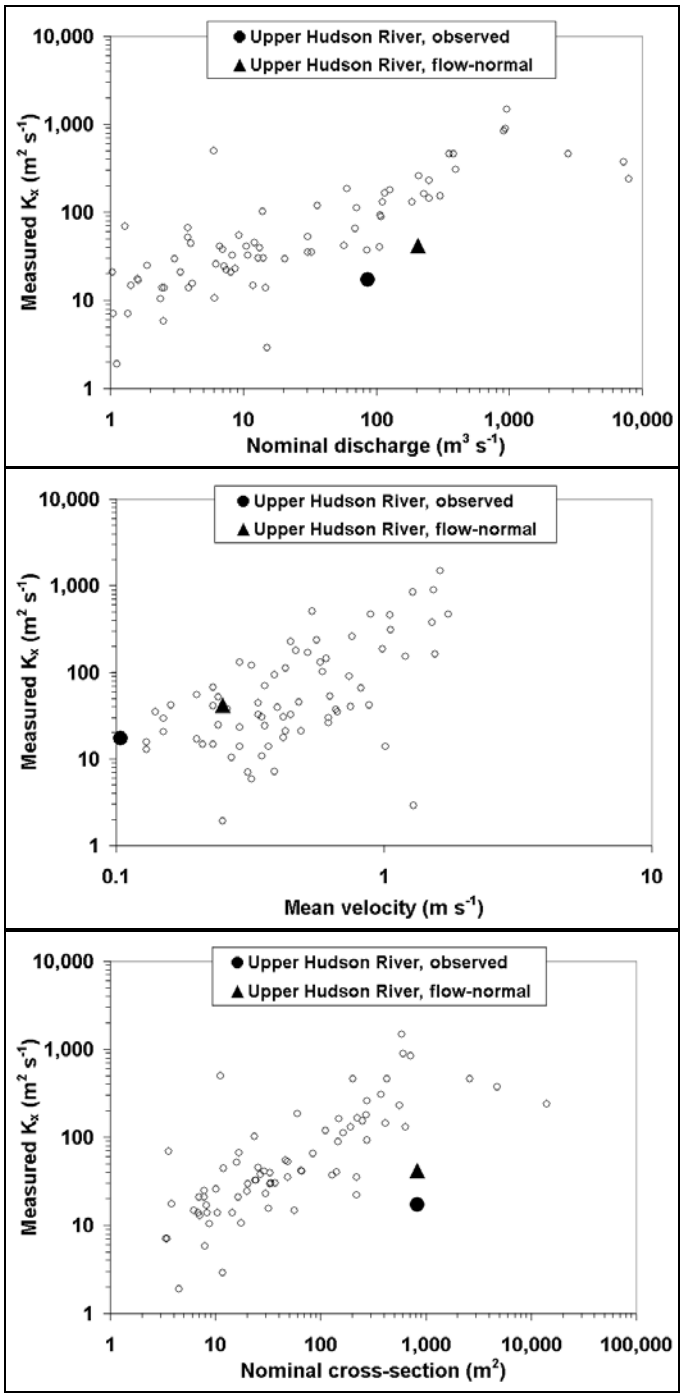

(single column figure)

Figure A1. ***Loss of SF_6 at broad-crested dams as a function of height at three different flow rates, corresponding to 50%, 100%, and 200% of the observed flow rates during the experiment.***

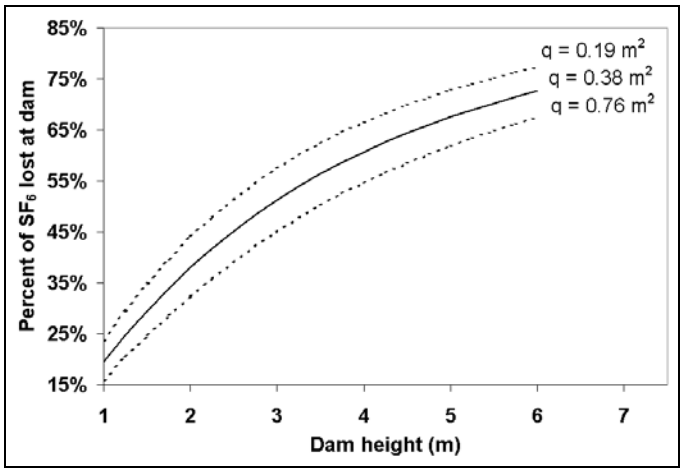

(single column figure)

Figure Captions

Figure 1. ***Map of the Study Area. Locations of dams are shown as horizontal bars. The inset reveals the canal (5 km long) above lock #6, where a small quantity of tracer was trapped for the duration of the experiment.***

Figure 2. ***SF_6 tracer concentrations and boat movement for a single, 6-hour profile on day 3. Note that the cross-sectional area of the main channel (leftmost peak) is approximately ten times larger than in the canals (center and rightmost peaks).***

*Figure 3****. Location of the peak SF_6 concentration vs. time, indicating a nearly constant advective rate of 9 km d^{-1}.***

Figure 4. ***Bi-directional SF_6 patch profiles on days 2 and 3. The longitudinal dispersion coefficient K_x was calculated for each of the surveys from σ^2 according to Equation (4), then averaged.***

Figure 5. ***Gaussian curves fit to 3 days of profiles in the canal above lock #6. All profiles shown are northbound. Average inventories from bi-directional profiles are shown above each curve.***

*Figure 6****. Variation of cross section and flow in the upper Hudson River*** *(bathymetry from EPA 2000).*

Figure 7. ***K_x versus (a) nominal discharge, (b) mean velocity, and (c) nominal cross-sectional area for the upper Hudson River, compared with data from Deng et al. (2001). The mean velocity used for the upper Hudson River was 0.10 m s^{-1} (from observed rate of tracer advection). Using this velocity yields a nominal discharge of 86.4 m^3 s^{-1}, somewhat higher than the monthly mean USGS observation at Ft. Edward. Filled circles represent observed values; filled triangles represent values corrected to long-term mean discharge (see text).***

Figure A1. ***Loss of SF_6 at broad-crested dams as a function of height at three different flow rates, corresponding to 50%, 100%, and 200% of the observed flow rates during the experiment.***

Keywords

Hudson River

River Mixing

Dispersion

Tracers

SF6

Sulfur hexafluoride

Gas Exchange

Dams

Advection

Water pollution